Journal of Membrane Science 329 (2009) 183–192

Contents lists available at ScienceDirect

Journal of Membrane Science

journal homepage: www.elsevier.com/locate/memsci

Modeling of oxygen scavenging for improved barrier behavior: Blend films

M.C. Ferrari[a,b], S. Carranza[a], R.T. Bonnecaze[a], K.K. Tung[a], B.D. Freeman[a], D.R. Paul[a,*]

[a] Department of Chemical Engineering, University of Texas at Austin, Austin, TX 78712, United States
[b] Dipartimento di Ingegneria Chimica, Mineraria e delle Tecnologie Ambientali Università di Bologna, Via Terracini 28, 40131 Bologna, Italy

ARTICLE INFO

Article history:
Received 11 November 2008
Received in revised form 15 December 2008
Accepted 17 December 2008
Available online 27 December 2008

Keywords:
Oxygen barrier
Scavenging
Mathematical modeling

ABSTRACT

The oxygen barrier behavior of polymer films can be significantly improved by incorporating particles of an oxygen-scavenging polymer, e.g., those based on butadiene containing an appropriate catalyst, in a matrix of a barrier polymer like poly(ethylene terephthalate) or polystyrene. This paper develops a mathematical model for predicting the transient barrier properties of such blend films. The analysis uses a "shrinking core" model for oxygen consumption by the particles and treats oxygen diffusion in the matrix polymer by a one-dimensional approximation. Scavenging can extend the time lag for the transient permeation by factors of thousands. A key point of the analysis is the calculation of the flux of oxygen exiting the downstream surface of the film for times of the order of the time lag and less using realistic geometrical and physical parameters.

1. Introduction

There is a well-recognized need for better polymer-based barrier materials for limiting oxygen ingression into food, beverages, pharmaceuticals, and particularly sensitive electronic components like displays based on organic light-emitting diodes. There has been a long effort to discover polymers with very low intrinsic permeability to oxygen and other small molecules. In recent years there has been much interest in incorporating plate-like particles into polymers that reduce permeability by making the penetrant diffusion path more tortuous. Each of these approaches seeks to reduce the oxygen transport in a steady-state situation.

Another approach that has been recognized since at least the 1960s is to greatly delay the time required to achieve steady-state transmission of the penetrant, i.e., to increase the time lag, θ, by scavenging or immobilizing the penetrant as it diffuses through the film [1–4]. The earliest examples involve adsorption by filler particles; however, in more recent times interest has turned to incorporation of reactive components, typically an oxygen-scavenging polymer or OSP, that irreversibly consume oxygen. This approach is specific to oxygen, and large quantities of oxygen can be consumed in this way. A number of patents have been issued describing variations on this idea for food and beverage packaging [5–11]. Polybutadiene is an example of a polymer that readily oxidizes [12–18] particularly in the presence of certain metal catalysts [19].

There are many ways an oxygen-scavenging polymer can be incorporated into a barrier film or sheet. One of the most straightforward ways is to simply blend a butadiene-containing polymer with a matrix polymer like poly(ethylene terephthalate), PET, or polystyrene, PS; however, owing to the immiscibility of these polymers, one can expect the oxygen-scavenging polymers to form particles (spherical in the simplest case) in the PET or PS matrix. In principle the particle size can be controlled by rheology and compounding conditions. Alternatively, the OSP may be co-extruded with the PET or PS to form a layered structure, perhaps with many layers [20]. In addition combinations of blends and co-extrusion may be used. The question becomes what is the optimal structure to achieve the best barrier performance while meeting the requirements of mechanical and optical properties. Clearly, there are many variables to consider with a very large experimental matrix to explore. A more rational approach would be to pursue an appropriate modeling strategy in combination with a more targeted experimental program. In the end, if the time to reach steady-state permeation is extended to ranges required by some applications, a totally experimental approach would be unworkable because individual experiments may take years to complete.

There has already been a considerable effort devoted to modeling this type of approach to improved barrier structures [1–3,21–33]. As it turns out, there are relatively simple and accurate schemes to predict the extent scavenging increases the time lag. However, for critical applications one needs to predict the extent of the "leakage" permeation that occurs during the period $t<\theta$, and this requires more sophisticated modeling as recognized by Nuxoll and Cussler [26]. We present here a modeling approach that attempts to address this issue for the case of a "blend" film as described above. The rate of oxygen consumption by the OSP

* Corresponding author. Tel.: +1 512 471 5392; fax: +1 512 471 0542.
E-mail address: drp@che.utexas.edu (D.R. Paul).

0376-7388/$ – see front matter © 2008 Elsevier B.V. All rights reserved.
doi:10.1016/j.memsci.2008.12.030

particles is needed as information input for these calculations. The rate of oxygen uptake by these particles involves a diffusional process in addition to reaction kinetics [34–38]. Here we simplify this process by applying a "shrinking core" approximation to the oxygen uptake of the OSP particles. Experimental techniques and results for quantifying the oxygen consumption by films of butadiene-containing polymers initiated as part of this program have recently been described [39,40].

A proposed model of the oxygen transport in the blended film is formulated here. A computer code has been developed to solve the resulting differential equations, and example calculations for typical parameters are presented to illustrate the effects that can be expected. Future work will focus on validation of the model and quantifying the various parameters by independent experiments.

2. Physical description of the model

Blend films of interest consist of a matrix polymer that is melt processible and a good oxygen barrier, e.g., PET, into which particles of a readily oxidizable polymer, such as ones based on butadiene, are dispersed. The size of the particles will be an issue and, within limits, can be varied by adjusting mixing conditions and rheological properties of the components. Invariably, there will be a distribution of particle sizes and possibly shapes; however, to simplify the model all the particles are considered to be spheres of the same radius R. Fig. 1 schematically illustrates a cross-sectional view of such a blend film. This film is assumed to have had no exposure to oxygen until ready for use; then at time $t = 0$ the upstream surface is exposed to a partial pressure of oxygen, $(p_{O_2})_0$, where in most cases this would be air so $(p_{O_2})_0 = 0.21$ kPa (or 0.21 atm). The downstream surface of the film is maintained at a low oxygen partial pressure, or for simplicity $(p_{O_2})_L \sim 0$. Oxygen is assumed to dissolve in the matrix polymer according to Henry's law at the upstream surface

$$C_m(0) = S_m(p_{O_2})_0 \tag{1}$$

where $C_m(0)$ is the concentration of oxygen in the matrix polymer phase at $x = 0$ and S_m is the effective solubility coefficient. Oxygen

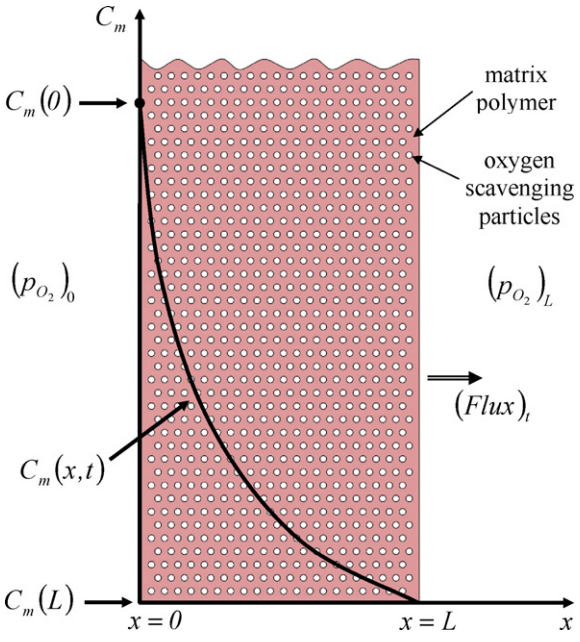

Fig. 1. Schematic illustration of a blend film containing particles of an oxygen-scavenging polymer in a matrix polymer.

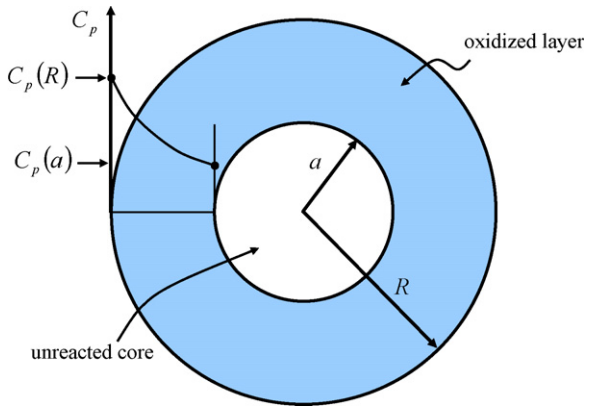

Fig. 2. Schematic illustration of the "shrinking core" model for oxygen diffusion and reaction within an oxygen scavenging particle.

diffuses in the matrix polymer according to Fick's law

$$\text{Flux} = -D_m \frac{\partial C_m}{\partial x} \tag{2}$$

Oxygen is consumed by the oxidizable particles; the kinetics of this process will be described by the shrinking core model illustrated in Fig. 2. Here it is assumed that at any given time each particle will have a completely oxidized shell, $R > r > a$, surrounding a completely unoxidized core, $a > r > 0$. This corresponds to the situation where diffusion through the oxidized particle medium is slow but the reaction is relatively fast. For a particle located in the film at position x (see Fig. 1), where the oxygen concentration in the matrix is $C_m(x,t)$, oxygen will partition into the oxidized surface according to

$$C_p(R) = \frac{C_m(x,t)}{H} \tag{3}$$

where $C_p(R)$ denotes the dissolved oxygen concentration in the oxidized polymer, H is a partition coefficient given by $H = S_m/S_p$, and S_p is the solubility coefficient for oxygen in the oxidized polymer. A reaction front exists at $r = a$ where oxygen reacts rather rapidly but according to a finite rate parameter, k, defined subsequently. The rate of oxygen arriving at this front, $r = a$, is controlled by oxygen diffusion through the oxidized shell with a diffusion coefficient, D_p.

A key element of this model is that C_m is assumed to be a continuously varying function of x only for a given time t. That is, we do not consider any variations in C_m in the y and z coordinate directions. Thus, the very complex three-dimensional composition field around a reactive particle is approximated by a much simpler one-dimensional problem. It is further assumed that the particles are sufficiently small that variations in C_m from the leading to the trailing surface of the particle are negligible. These simplifications along with the "shrinking core" approach for dealing with oxygen consumption within particles make the mathematical aspects of the model more tractable; however, these are the limitations that must eventually be tested by experiment and other modeling approaches before full confidence can be vested in the type of predictions given here.

This physical picture is developed into a complete mathematical model in the next section.

3. Mathematical formulation of the model

For any oxygen-scavenging polymer (OSP) particle at an arbitrary location, x, in the film, the shrinking core approach suggested in Fig. 2 considers the reaction to be fast compared to the diffusion process in the particle shell so that when oxygen reaches the surface

of the core it reacts immediately. Due to the reaction, the scavenging material is consumed, and the radius of the reactive core of the OSP decreases with time; meanwhile the shell of reacted material around the core becomes thicker.

A simple steady-state balance can be used to approximate the concentration profile inside the shell of reacted material to yield,

$$\frac{D_p}{r^2}\frac{d}{dr}\left(r^2\frac{dC_p}{dr}\right)=0 \tag{4}$$

where D_p is the diffusion coefficient in the oxidized OSP. Integrating Eq. (4) twice and applying the boundary conditions shown in Fig. 2, i.e.,

$$\begin{aligned} C_p &= C_p(R)=\frac{C_m(x,t)}{H} \quad \text{at } r=R,\\ C_p &= C_p(a) \quad \text{at } r=a, \end{aligned} \tag{5}$$

the concentration profile in the shell can be obtained for a given concentration $C_p(R)$ at the particle surface is given by

$$C_p(r)=C_p(R)-\frac{C_p(R)-C_p(a)}{(1-(R/a))}\left(1-\frac{R}{r}\right) \tag{6}$$

where H is the oxygen partition coefficient between the matrix and the reacted surface. According to Fick's law, the radial oxygen flux within the OSP is given by

$$N=-D_p\frac{dC_p}{dr}=-D_p\frac{C_p(R)-C_p(a)}{((R/a)-1)}\left(\frac{R}{r^2}\right) \tag{7}$$

Assuming the rate of reaction is fast relative to the rate of diffusion, the flux of oxygen at the reaction front ($r=a$) can be equated to the rate of oxygen consumption at $r=a$ which is approximated by a simple first order surface reaction. Thus,

$$-D_p\frac{dC_p}{dr}=-kC_p(a) \tag{8}$$

Combining Eqs. (7) and (8), the concentration of dissolved oxygen at the reaction front, $C_p(a)$, can be expressed as

$$C_p(a)=\frac{C_p(R)}{1+(ka^2/D_pR)((R/a)-1)} \tag{9}$$

The Rate of Oxygen Consumption, ROC, for the single particle can be calculated as the product of the flux of oxygen and the surface area at $r=a$

$$\mathrm{ROC}=4\pi a^2kC_p(a)=4\pi a^2k\frac{C_p(R)}{1+(ka^2/RD_p)((R/a)-1)} \tag{10}$$

A simple mass balance relates the time profile of the un-reacted core radius to the ROC

$$\frac{d}{dt}\left(\rho_{\mathrm{polymer}}\frac{4\pi a^3}{3}\right)=-\frac{\mathrm{ROC}}{\beta}\rho_{\mathrm{polymer}} \tag{11}$$

where β takes into account the capacity of the particle to consume oxygen when fully oxidized; this parameter is defined as the moles of oxygen consumed per unit volume of OSP and can be determined by experimentally measuring the mass uptake of the OSP alone [39,40]. Combining Eqs. (10) and (11) and simplifying leads to the following dynamic equation for the radius of unreacted OSP particles

$$\frac{da}{dt}=-\frac{kC_p(R)/\beta}{1+(ka^2/RD_p)((R/a)-1)} \tag{12}$$

It must be remembered that $C_p(R)$ is a function of x and t, see Eq. (5); so it is implicitly assumed that this model describes a situation where the particle boundary condition varies with time.

It is now possible to consider the complete membrane consisting of particles dispersed within the matrix, see Fig. 1. A continuum approach, assuming that the particles are sufficiently small, numerous, and well dispersed, is used where all properties and variables are averages over a particular film volume. The transport of oxygen through the membrane can be described considering the Fickian diffusion in the matrix and the consumption due to the reaction within the particle. The latter term can be calculated from the ROC of a single particle multiplied by the number density, ρ, of particles in the film

$$\rho=\frac{3\phi}{4\pi R^3} \tag{13}$$

where ϕ is the volume fraction of particles of radius R. The resulting diffusion equation is given by

$$\frac{\partial C_m}{\partial t}=D_m\frac{\partial^2C_m}{\partial x^2}-\frac{3\phi}{R^3}\cdot a^2\cdot k\cdot\frac{C_m}{H}\cdot\left[1+\frac{ka^2}{RD_p}\left(\frac{R}{a}-1\right)\right]^{-1} \tag{14}$$

This equation must be solved simultaneously with the following equations describing the decrease in the radius of the unreacted core, a, of scavenging particle for all x and t.

$$\frac{da}{dt}=\begin{cases}-\dfrac{kC_m}{\beta H}\left[1+\dfrac{ka^2}{RD_p}\left(\dfrac{R}{a}-1\right)\right]^{-1} & \text{for } a\geq 0\\ 0 & \text{for } a=0\end{cases} \tag{15}$$

This system of equations must be solved for the following initial and boundary conditions, representing the transient permeation experiment:

$$\text{IC}: \quad C_m(x,t=0)=0, \qquad a(x,t=0)=R \tag{16}$$

$$\begin{aligned}\text{BC}: \quad & C_m(0)\equiv C_m(x=0,t)=S_mp_{O_2},\\ & C_m(L)\equiv C_m(x=L,t)=0\end{aligned} \tag{17}$$

The equations can be expressed in a more convenient non-dimensional form by defining the following dimensionless variables

$$\tilde{C}=\frac{C}{C_m(0)}, \qquad \tilde{x}=\frac{x}{L}, \qquad \tilde{a}=\frac{a}{R}, \qquad \tilde{t}=\frac{t}{L^2/D} \tag{18}$$

The differential equations plus initial and boundary conditions become

$$\frac{\partial\tilde{C}}{\partial\tilde{t}}=\frac{\partial^2\tilde{C}}{\partial\tilde{x}^2}-3\phi\frac{(Da)\Delta}{\varepsilon^2H}\left[\frac{\tilde{a}^2}{1+(Da)(\tilde{a}-\tilde{a}^2)}\right]\tilde{C} \tag{19}$$

$$\begin{aligned}&\text{IC}: \quad \tilde{C}(\tilde{x},\tilde{t}=0)=0\\ &\text{BC}: \quad \tilde{C}(\tilde{x}=0,\tilde{t}>0)=1, \qquad \tilde{C}(\tilde{x}=1,\tilde{t}>0)=0\end{aligned} \tag{20}$$

$$\frac{d\tilde{a}}{d\tilde{t}}=\begin{cases}-\dfrac{C_m(0)}{\beta}\dfrac{(Da)\Delta}{\varepsilon^2H}\left[\dfrac{1}{1+(Da)(\tilde{a}-\tilde{a}^2)}\right]\tilde{C} & \text{for } \tilde{a}>0\\ 0 & \text{for } \tilde{a}=0\end{cases} \tag{21}$$

$$\text{IC}: \quad \tilde{a}(\tilde{x},\tilde{t}=0)=1 \tag{22}$$

where $(Da)=kR/D_p$ is the Damköhler number for the OSP particle, i.e., the ratio between the time scale of diffusion and the time scale of reaction, $\varepsilon=R/L$ is the ratio of the radius of the OSP and the film thickness, and $\Delta=D_p/D_m$ is the ratio of the diffusion coefficient of the OSP to the diffusion coefficient of the film matrix. The term $C_m(0)$ is the concentration of oxygen in the matrix at the upstream surface of the membrane and was defined in Eq. (16). Note that the product $C_m(0)/\beta$ is dimensionless.

The non-dimensional Eqs. (19) and (21) were solved numerically using an explicit finite difference method. The equations were discretized using a three-point central difference for the spatial derivatives and two point forward difference for the time derivatives. For this problem, the early transient as well as steady-state behavior are of interest. The numerical solution utilized variable

time steps to capture the behavior over the entire time span while keeping computational times within practical limits. While the numerical solution was developed in MatLab for convenient matrix manipulation, it did not rely on any specialized solvers. When there are no reactive particles in the matrix, the solution should reduce to the classical transient diffusion in a membrane film; the numerical results for the case with no particles was found to be in excellent agreement with the analytical solution given by Crank [41].

The solution of Eqs. (19) and (21) provides space and time profiles for the dimensionless oxygen concentration, $\tilde{C}(\tilde{x}, \tilde{t})$, and the dimensionless radius of the unreacted core of the OSP particles, $\tilde{a}(\tilde{x}, \tilde{t})$. For barrier applications, it is important to know the time evolution of the oxygen flux and the cumulative amount of permeate, Q_t, exiting the downstream surface of the barrier film. Both quantities can be derived from the concentration profile. The flux is given by

$$(\text{Flux})_t \equiv N(x = L, t) = -D_m \left.\frac{dC}{dx}\right|_{x=L} = -D_m \frac{C_m(0)}{L} \left.\frac{d\tilde{C}}{d\tilde{x}}\right|_{\tilde{x}=1} \quad (23)$$

$$\tilde{N}\big|_{\tilde{x}=1} = \frac{(\text{Flux})_t}{(\text{Flux})_{ss}} = -\left.\frac{d\tilde{C}}{d\tilde{x}}\right|_{\tilde{x}=1} \quad (24)$$

where $D_m C_m(0)/L$ is the flux at steady state. The cumulative amount of permeate is given by

$$Q_t = \int_0^t N\big|_{x=L}\, dt$$

$$= (\text{Flux})_{ss} \frac{L^2}{D_m} \int_0^{\tilde{t}} -\left.\frac{d\tilde{C}}{d\tilde{x}}\right|_{\tilde{x}=1} d\tilde{t} = (\text{Flux})_{ss} 6\theta_0 \int_0^{\tilde{t}} -\tilde{N}\big|_{\tilde{x}=1}\, d\tilde{t} \quad (25)$$

$$\frac{Q_t}{(\text{Flux})_{ss}\theta_0} = 6 \int_0^t -\left.\frac{d\tilde{C}}{d\tilde{x}}\right|_{\tilde{x}=1} d\tilde{t} = 6 \int_0^{\tilde{t}} -\tilde{N}\big|_{\tilde{x}=1}\, d\tilde{t} \quad (26)$$

where $\theta_0 = L^2/6D_m$ is the diffusion time lag for the matrix without any OSP. From the dimensionless equations we see that $\tilde{C}$ is a function of $\tilde{x}$ and $\tilde{t}$ plus the dimensionless parameters ϕ, $C_m(0)/\beta$, Δ, ε, H and (Da). Consequently, $(\text{Flux})_t/(\text{Flux})_{ss}$ and $Q_t/((\text{Flux})_{ss}\theta_0)$ are functions of $\tilde{t}$ and the same dimensionless parameters.

The dimensionless flux presented in the results section was obtained numerically from Eq. (24) using the five-point backward difference at $\tilde{x} = 1$. The dimensionless oxygen permeate was obtained numerically from Eq. (26) using the trapezoidal rule for integration. Note that the dimensionless time used in the derivation is defined as $\tilde{t} = t/(L^2/D)$; however, for comparison with diffusion time scales, all graphs presented in the results section use $t/\theta_0 = 6\tilde{t}$.

4. Model parameter ranges

The mathematical model described in the previous section contains numerous parameters, see summary in Table 1, that must be determined or specified to make the model predictive. These parameters are discussed here with some selections made for the purpose of showing example predictions in the next section.

The thickness, L, of typical barrier film or sheet would generally be in the range 50–500 μm. Based on much experience, one can expect that polymer particles dispersed in a polymer matrix prepared by melt compounding and extrusion would have diameters in the range of 1–10 μm or radii, R, of 0.5–5 μm [42]. The volume fraction, ϕ, of these particles in the blend might be expected to be within the range of 0.05–0.20.

A typical matrix polymer might be poly(ethylene terephthalate), PET, which is used extensively for conventional barrier applications. Published values of S_m and D_m for PET from the literature [43] are shown in Table 1. Values for polystyrene, which is not such a good barrier material, are also included in Table 1. As of yet, there are no reported values of S_p and D_p for butadiene-based polymers (the oxygen-scavenging polymer of interest here) in the fully oxidized state. Since the fully oxidized material is hard and glassy, one could expect S_p to be similar to S_m. Efforts are underway currently to evaluate S_p, D_p and k from oxygen uptake experiments like those recently published [39,40]; an analysis of such data will be the subject of a forthcoming publication. For now, Table 1 includes some preliminary estimates of the ranges of D_p and k from this type of analysis. The parameter β characterizes the ultimate oxygen scavenging capacity of the butadiene-based polymer, which has been found experimentally to be in the range of 8–32% by weight. The values of β in Table 1 reflect this range in the units shown.

Table 1
Range of model parameters of interest.

Parameter	Estimated range	Base case for calculations	Ref
L	50–500 μm	250 μm	
R	0.5–5 μm	2.5 μm	
ϕ	0.05–0.20	0.1	
S_m	0.097 cm^3(STP)/cm^3 mpa for PET	0.097 cm^3(STP)/cm^3 mpa	[43]
	1.9 cm^3(STP)/cm^3 mpa for PS		[44]
D_m	5.6×10^{-9} cm^2/s for PET	5.6×10^{-9} cm^2/s	[43]
	1.0×10^{-7} cm^2/s for PS		[44]
S_p	Measurements needed, probably ~ S_m	0.098 cm^3(STP)/cm^3 atm	
D_p	Estimated to be ~$(1–6) \times 10^{-9}$ cm^2/s	2×10^{-9} cm^2/s	
k	Estimated to be 10^{-5} to 10^{-3} cm/s	8×10^{-5} cm/s	
β	$(2.5–10) \times 10^{-3}$ mol O_2/cm^3 OSP	4×10^{-3} mol O_2/cm^3 OSP	
$H = S_m/S_p$	~1	1	
$\varepsilon = R/L$	10^{-3} to 50×10^{-3}	10^{-2}	
$\Delta = D_p/D_m$	10^{-2} to 100	2/5.6 for PET	
$Da = kR/D_p$	*0.1 to 500*	*10*	

The physical parameters described above were used to estimate the range of values the various dimensionless groups in the model, see Eqs. (18)–(22), might be expected to have. Table 1 also lists a "base case" set of parameters that will be used in the next section to illustrate the model predictions; this case considers PET as the matrix and uses mid-range values of the geometrical parameters. Some of the calculations shown later illustrate the effects of varying some of these parameters from the base case.

For reference, the diffusion time lag for a PET film with a thickness of 250 μm without scavenging particles would be $\theta_0 = (L^2/6D_m) \sim 5.2$ h. For polystyrene, θ_0 at this thickness would be only 0.3 h.

It should be noted that in this model, the physical effects of the particles on the oxygen diffusion process has been ignored. In the extreme case, the particles might be considered impermeable in which case Maxwell's equation [45] would predict the following relationship between the steady-state permeability of the blend, P_{blend}, to that of the matrix, P_m

$$\frac{P_{blend}}{P_m} = \frac{1 - \phi}{1 - \phi/2} \quad (27)$$

which for $\phi = 0.2$ amounts to about an 11% reduction for the blend. This is of no consequence for the current considerations.

5. Example calculations

In this section, numerical calculations made using the procedures described are shown to illustrate the predictions of the model developed above. The model involves a considerable parameter space so the strategy here is to use the "base case" values listed in Table 1 and then systematically explore the trends produced by varying each parameter individually within the "estimated range" shown in Table 1; however, it is instructive to examine cases when the rate parameter k is outside this range.

Fig. 3 explores the effect of varying the loading of oxygen-scavenging polymer in a matrix of poly(ethylene terephthalate) or PET. Fig. 3(a) shows results in terms of the dimensionless cumulative amount of oxygen exiting the downstream surface of the film versus dimensionless time (defined here as t/θ_0) for several values of ϕ all plotted on arithmetic coordinates. After an initial transient period, a linear asymptote is approached which can be extrapolated to the time axis to define the time lag θ with scavenging. Note that scavenging extends the time lag by several thousand-fold. However, such plots do not give a full picture of what is happening for times less than θ; as explained earlier, the "leakage" through the film for $t < \theta$ is of great interest. To see this, it is useful to plot the oxygen flux

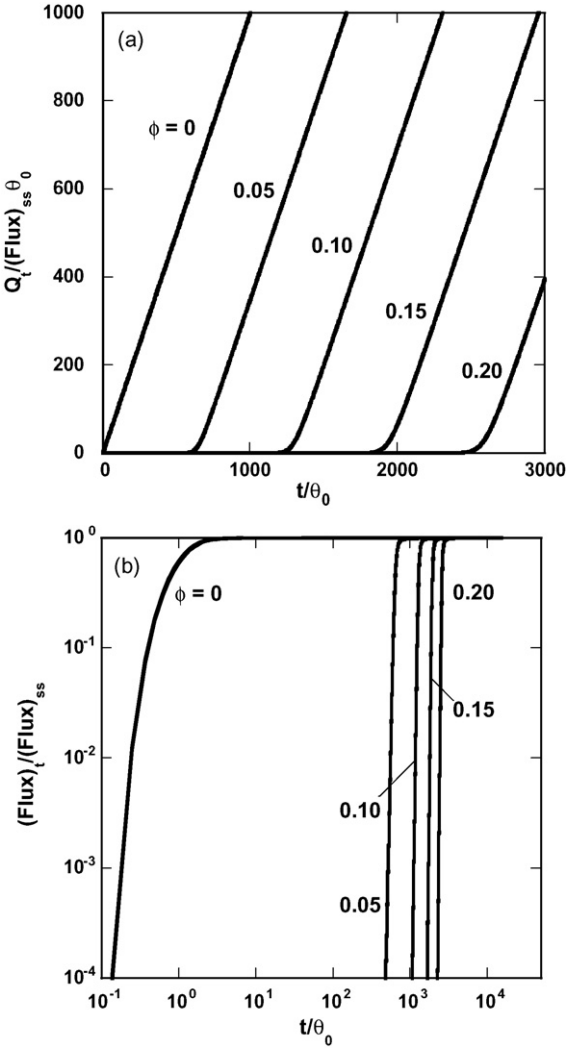

Fig. 3. Predicted transient permeation behavior for a blend film containing various volume fractions of oxygen-scavenging polymer shown as (a) cumulative amount of oxygen and (b) flux of oxygen exiting the downstream film surface. All parameters set at base case values (see Table 1) except for ϕ as noted.

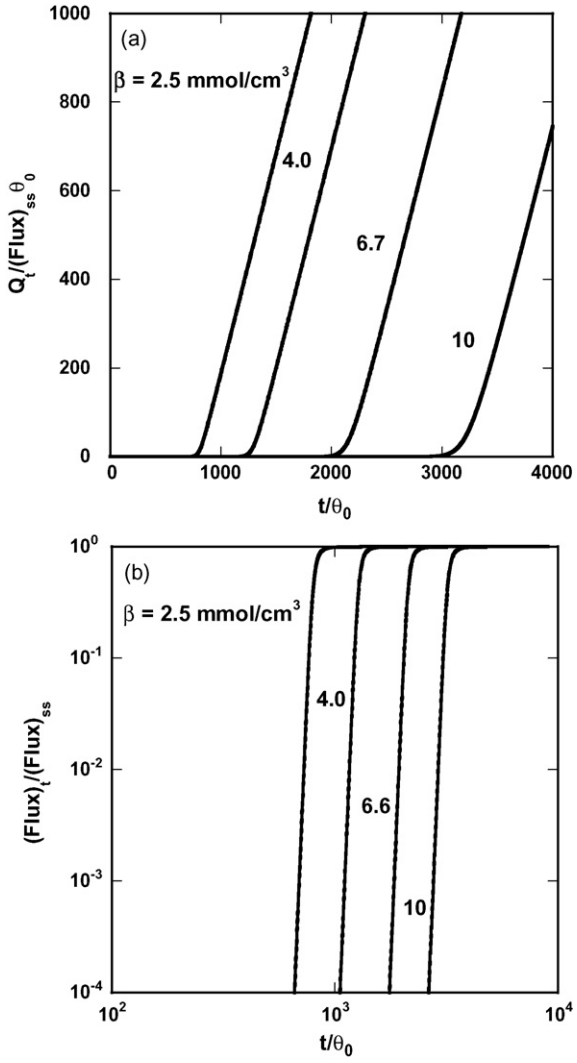

Fig. 4. Predicted transient permeation behavior for a blend film containing various volume fractions of the oxygen reaction capacity of the oxygen-scavenging polymer shown as (a) cumulative amount of oxygen and (b) flux of oxygen exiting the downstream film surface. All parameters set at base case values (see Table 1) except for β as noted; β is given in units of millimoles O_2/cm^3 OSP.

exiting the film normalized by the steady-state value on a logarithmic scale versus time, also on a dimensionless logarithmic scale, as shown in Fig. 3(b). In this case, the fluxes for times $t < \theta$ are at least 10^{-4} times smaller than the steady-state values. However, as seen later, this may not always be the case.

Fig. 4 shows analogous plots as in Fig. 3 where β is varied rather than ϕ. Increasing the capacity of the oxygen-scavenging polymer to take up oxygen for a fixed loading $\phi = 0.10$ by increasing β has somewhat similar effects as increasing ϕ.

Interestingly, the asymptotic solutions illustrated in Fig. 3(a) and Fig. 4(a), and consequently θ, are independent of the kinetics of the scavenging reactions and all the parameters that affect the rate of reaction. Thus, θ/θ_0 depends only on the capacity to absorb oxygen, ϕ and β, and the solubility of oxygen in the polymer matrix or $C_m(0)$. As shown in the Appendix, the method of Frisch [46] can be used to develop the following analytical expression for θ/θ_0

$$\frac{\theta}{\theta_0} = 1 + \frac{3\beta}{C_m(0)} \tag{28}$$

Siegel and Cussler [24] developed an analogous relationship for a somewhat different scavenging model.

Fig. 5 shows how the time lag relative to the case of no scavenging depends on ϕ and β for PET (part a) and PS (part b) matrices calculated by numerical solution of the model described above; these values of θ/θ_0 are in excellent agreement with those calculated by Eq. (28). These plots are linear and could be collapsed into master plots for all matrix polymers using the dimensionless ratio $C_m(0)/\beta$ rather than β as the parameter, as predicted by Eq. (28). Note that owing to the lower solubility of oxygen in PET than PS, see Table 1, the extension of the time lag caused by scavenging is greater for PET than PS by almost a factor of two. Of course, what happens during the times less than θ can be critically dependent on factors affecting the rate of oxygen consumption. This is the main focus on what follows.

Fig. 6 shows responses for the base case as the reaction rate parameter k is varied in a range of values much lower than what preliminary experiments suggest would be reasonable. For this case, $\theta/\theta_0 \sim 1250$ and all the plots of the cumulative amount of oxygen exiting the film downstream surface versus time would eventually approach a single asymptote, except of course, for the case of no scavenging ($k = 0$). Clearly, the approach to this asymptote depends strongly on k. This "leakage" is better seen by examining the flux versus time using logarithmic scales. Such flux plots, see Fig. 6(b), show two rapid rises; the first occurs at times of the order of θ_0 and the second at times of order of θ with a plateau region between these limits. The value of the flux relative to the steady-state case is lower the larger the value of k, i.e., the faster the scavenging reaction. Note that these plateaus are only seen for values of k that are at least an order of magnitude less than the expected range listed in Table 1. Of course, whether a plateau is seen or not depends on the lower limit chosen for the flux scale, which has been set at 10^{-4} here. Similar plateaus would be seen in Figs. 3(b) and 4(b) had this limit been set at lower values.

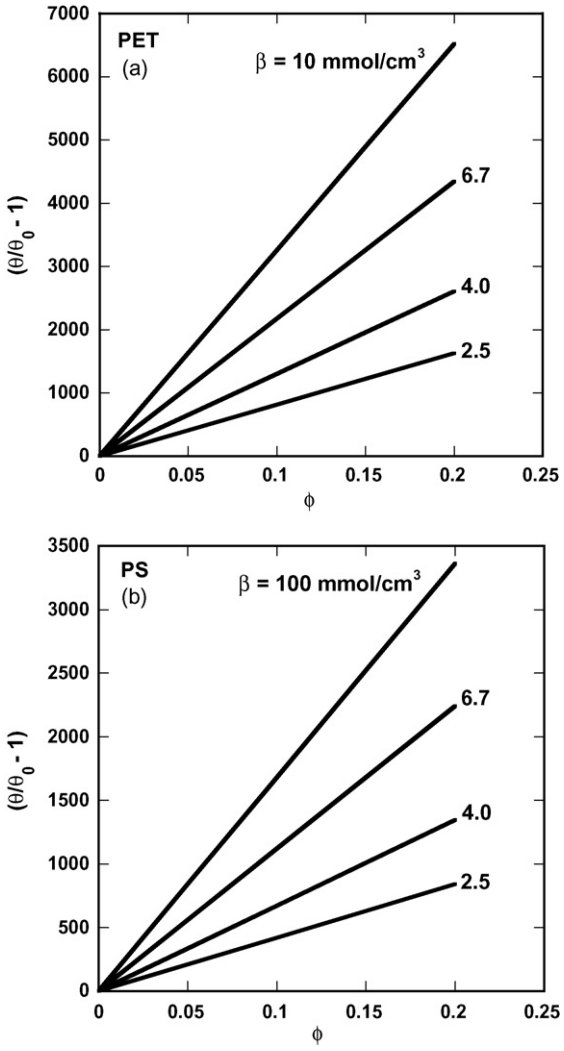

Fig. 5. Predicted extension of the transient permeation time lag, θ, caused by scavenging as function of ϕ and β for (a) poly(ethylene terephthalate) and (b) polystyrene as the matrix polymer. All parameters set at base case values (see Table 1) except as shown.

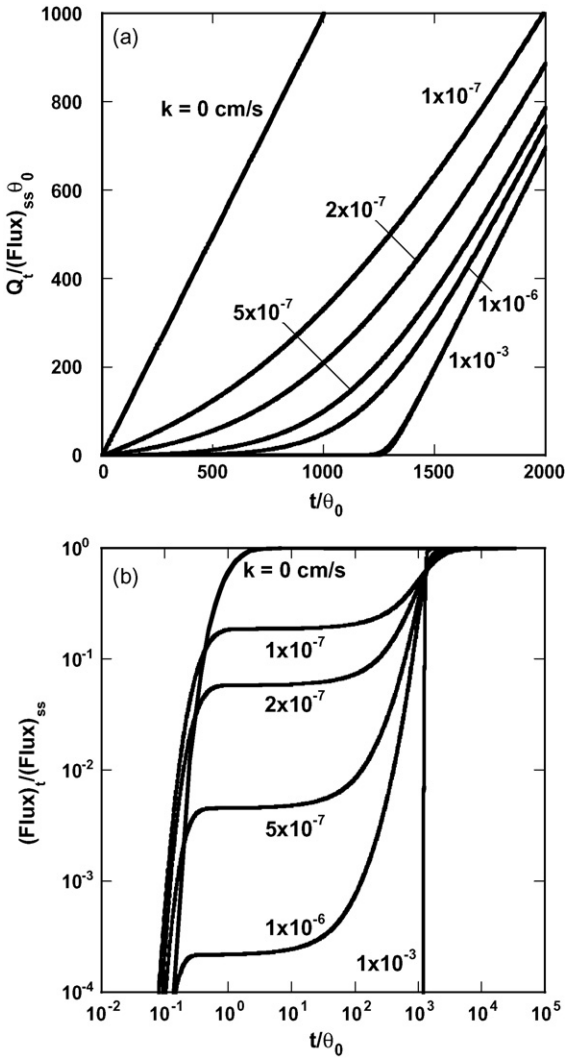

Fig. 6. Predicted transient permeation behavior for a blend film for different values of the oxygen scavenging rate parameter shown as (a) cumulative amount of oxygen and (b) flux of oxygen exiting the downstream film surface. All parameters set at base case values (see Table 1) except for k as noted.

Fig. 7 shows for the base case, on a more expanded time scale near $t \sim \theta$ and beyond, how the size of the oxygen-scavenging polymer particles, R, affects the flux of oxygen exiting the film. For a given time, the flux increases as the particles become larger owing to the coupling of mass transfer within the particle with the reaction, see Fig. 2. Clearly, there is some advantage to having the OSP finely dispersed in the matrix polymer.

Fig. 8(a) shows for the base case how varying the overall film thickness, L, affects the dimensionless flux at a given dimensionless time. Interestingly, the dimensionless flux becomes larger as the film becomes thinner. In simple terms, the time scale for diffusion is proportional to L^2 but the time scale for reaction does

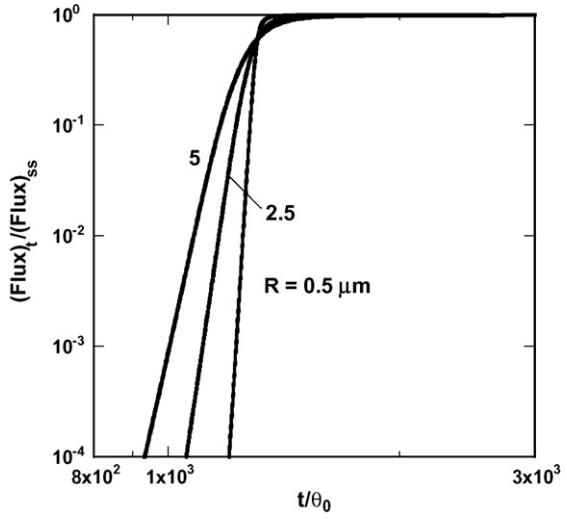

Fig. 7. Predicted effect of oxygen-scavenging polymer particle radius on the flux of oxygen exiting the blend film. All parameters set at base case values (see Table 1) except R as noted.

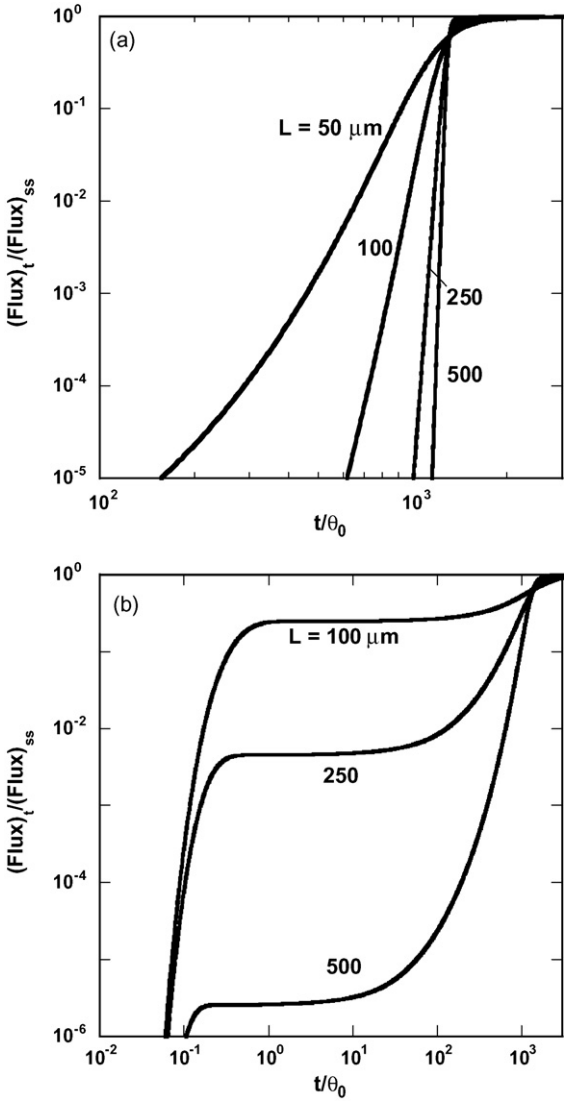

Fig. 8. Predicted effect of blend film thickness on oxygen flux exiting the downstream surface for (a) $k = 8 \times 10^{-5}$ cm/s (note expanded time scale) and (b) $k = 5 \times 10^{-7}$ cm/s. All other parameters set at base case values (see Table 1) except L as noted.

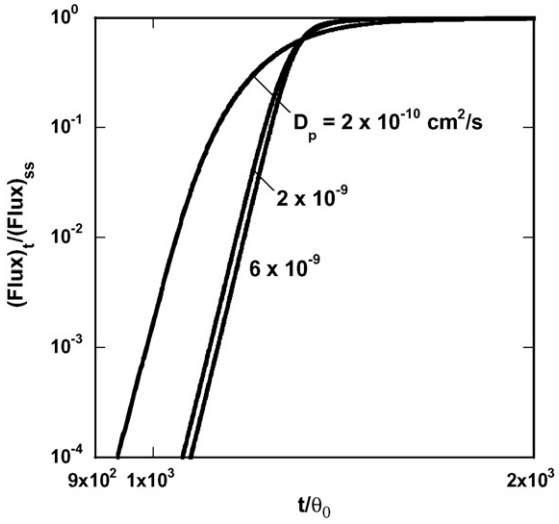

Fig. 9. Predicted effect of diffusion coefficient in the oxidized layer of the oxygen scavenging particle on the oxygen flux exiting the downstream surface of the blend film. All parameters set at base case values (see Table 1) except for D_p as noted.

not depend on L; thus, for thinner films there is less time for the scavenging reaction to occur before oxygen breakthrough. However, in interpreting these dimensionless plots it is important to remember that $(Flux)_{ss} \sim L^{-1}$ and $\theta_0 \sim L^2$. As the value of k becomes lower the extent of "leakage" in the time range $\theta_0 < t < \theta$ relative to $(Flux)_{ss}$ becomes more significant and strongly dependent on L as illustrated in Fig. 8(b) for $k = 5 \times 10^{-7}$ cm/s for various values of L with all other parameters corresponding to the base case. The effect on the absolute flux leakage is even greater since $(Flux)_{ss} \sim L^{-1}$.

The effect of the diffusion coefficient within the oxidized layer of the butadiene containing particles, D_p, over the expected range of values $(2–6) \times 10^{-9}$ cm²/s, see Table 1, turns out to be very small as illustrated in Fig. 9 where the dimensionless flux is plotted versus an expanded time scale in the vicinity of θ. Reducing the values of D_p by and order of magnitude to 2×10^{-10} cm²/s produces a more noticeable effect, as seen in Fig. 9. Overall, D_p is not a very influential parameter in the barrier performance of blend films as represented by this model.

As a final issue, the effect of varying the matrix polymer is explored by comparing the performance of films based on PS versus PET as the matrix; all the parameters are kept the base case values given in Table 1 except for changing S_m and D_m to the values for PS. Because of the higher oxygen solubility in PS, the dimensionless time lag θ/θ_0 is smaller for PS than PET, see Fig. 10(a); of course, because of the higher D_m of PS than PET, the value of θ_0 is about 18 times smaller for PS than PET. Considering the effect of both S_m and D_m, the absolute value of θ for PET is about 37 times that of PS. Furthermore, the slope of the dimensionless flux–time plots for PET is much steeper than for PS in the region of θ, see Fig. 10(b). PS is prone to show greater "leakage" permeation in the region $t < \theta$ than PET.

The effects illustrated quantitatively above by actual numerical solution of the model equations can be understood qualitatively, within certain limitations, by examining the scavenging terms in the model, i.e., the last term in Eq. (19) and Eq. (21) for $\tilde{a} < 0$. As seen earlier, θ/θ_0 is a function of ϕ and $C_m(0)/\beta$ only, and they affect the outcome in opposite directions. Increasing $C_m(0)/\beta$, which appears only in Eq. (21) accelerates the rate of change of the shrinking core radius, a, and results in a decrease of θ/θ_0. Conversely, increasing ϕ, which appears only in Eq. (19), accelerates the rate of change of the oxygen concentration, $\tilde{C}$, and results in an increase of θ/θ_0. The

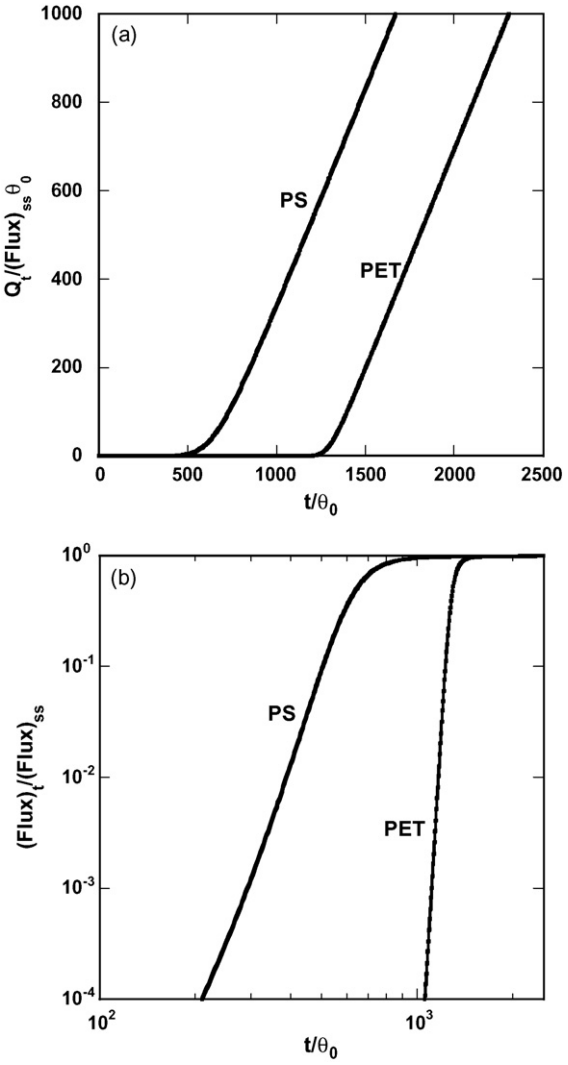

Fig. 10. Comparison of predicted transient permeation behavior for poly(ethylene terephthalate) versus polystyrene as the matrix polymer shown as (a) cumulative amount of oxygen and (b) flux of oxygen exiting the downstream surface of blend film. All parameters set at base case values (see Table 1) except as needed for polystyrene.

constant factor

$$\frac{(Da)\Delta}{\varepsilon^2 H} = \frac{kR}{D_p}\frac{D_p}{D_m}\frac{L^2}{R^2}\frac{1}{H} = \frac{kL^2}{RD_m H} = (Da)_{eff} \tag{29}$$

where $(Da)_{eff}$ is an effective Damköhler number, appears in both Eqs. (19) and (21) and plays a dominant role in the extent of leakage flux prior to reaching the asymptotic steady-state flux. However, the first defined Damköhler number, (Da), appears in the variable term in braces, and plays a more limited role since it is damped by the $(\tilde{a} - \tilde{a}^2)$ term. In general, the extent of leakage flux prior to reaching the asymptotic steady-state flux can be reduced by making choices (materials, formulation, and geometry) that maximize the term $\phi(Da)_{eff}$.

6. Summary and conclusions

A model has been developed for predicting the oxygen barrier behavior of a blend film containing particles of an oxygen-scavenging polymer, e.g., polymers containing butadiene segments, dispersed in a matrix polymer. It is assumed that the oxygen scavenging by the particles can be described by a "shrinking core" model while the diffusion of oxygen in the matrix can be approximated as a function only of the coordinate axis in the thickness direction and of time. The model equations have been solved numerically for the cases where the matrix polymer is either poly(ethylene terephthalate) or polystyrene for values of the geometric and physical parameters that are believed to be realistic in order to show how barrier behavior is affected by each one. Scavenging extends the time lag, θ, for transient permeation by a factor that depends only on the loading of the oxygen-scavenging polymer and its capacity to consume oxygen relative to the capacity of the matrix polymer to dissolve oxygen; the time lag can easily be extended by factors of thousands. However, for demanding applications like displays based on organic light-emitting diodes, the flux of oxygen exiting the downstream surface of the film on time scales of the order of θ and less may be the limiting criteria for the utility of this technology. This model was used to estimate this leakage flux for $t < \theta$, which depends on the factors that affect the rate of oxygen consumption relative to the rate of oxygen diffusion and can be summarized in terms of an effective Damköhler number.

Future work will focus on more detailed analysis of the kinetics of oxygen scavenging by polymers based on butadiene experimental validation of the current model for blend films, and extension of this approach to barrier materials using layered polymer films. Longer range, it would be important to consider scavenging concepts for other species like water and carbon dioxide.

Acknowledgments

This work was supported by the National Science Foundation under Grant No. DMR0423914 and by a visiting fellowship from the Graduate Program of the University of Bologna.

Appendix A

The time lag for the blend film modeled in this paper can be predicted analytically by adapting the asymptotic analysis developed by Frisch [46] for diffusion time lag, and more recently employed by Siegel and Cussler [24] for prediction in reactive membrane films.

Combining and rearranging dimensionless Eq. (19) for concentration and (21) for radius $\tilde{a} > 0$ gives

$$\frac{\partial \tilde{C}}{\partial \tilde{t}} - \frac{3\phi\beta}{C_m(0)}\tilde{a}^2\frac{d\tilde{a}}{d\tilde{t}} = \frac{\partial^2 \tilde{C}}{\partial \tilde{x}^2} \tag{A.1}$$

Integrating Eq. (A.1) from an arbitrary position along the film, $\tilde{x}$, to 1 gives

$$\int_{\tilde{x}}^{1}\left[\frac{\partial \tilde{C}}{\partial \tilde{t}} - \frac{\phi\beta}{C_m(0)}\frac{\partial \tilde{a}^3}{\partial \tilde{t}}\right] dy = \left.\frac{\partial \tilde{C}}{\partial \tilde{x}}\right|_1 - \frac{\partial \tilde{C}}{\partial \tilde{x}} \tag{A.2}$$

Integrating again in space, now from 0 to 1 gives

$$\int_0^1\int_{\tilde{x}}^{1}\left[\frac{\partial \tilde{C}}{\partial \tilde{t}} - \frac{\phi\beta}{C_m(0)}\frac{\partial \tilde{a}^3}{\partial \tilde{t}}\right] dy\, d\tilde{x} = \left.\frac{\partial \tilde{C}}{\partial \tilde{x}}\right|_1\int_0^1 d\tilde{x} - \int_0^1\frac{\partial \tilde{C}}{\partial \tilde{x}}\, d\tilde{x} \tag{A.3}$$

Note that double integrals on the left hand side can be simplified to a single integral, by reversal of the integration order. Simplifying the left hand side and evaluating the right hand side, Eq. (A.3) becomes

$$\int_0^1 \tilde{x}\left[\frac{\partial \tilde{C}}{\partial \tilde{t}} - \frac{\phi\beta}{C_m(0)}\frac{\partial \tilde{a}^3}{\partial \tilde{t}}\right] d\tilde{x} = \left.\frac{\partial \tilde{C}}{\partial \tilde{x}}\right|_1 - \tilde{C}(1,\tilde{t}) + \tilde{C}(0,\tilde{t}) = \left.\frac{\partial \tilde{C}}{\partial \tilde{x}}\right|_1 + 1 \tag{A.4}$$

Integrating Eq. (A.4) over time results in the following

$$\int_0^{\tilde{t}}\int_0^1 \tilde{x}\left[\frac{\partial\tilde{C}}{\partial\tilde{t}} - \frac{\phi\beta}{C_m(0)}\frac{\partial\tilde{a}^3}{\partial\tilde{t}}\right]d\tilde{x}\,d\tilde{t} = \int_0^{\tilde{t}}\left.\frac{\partial\tilde{C}}{\partial\tilde{x}}\right|_1 d\tilde{t} + \int_0^{\tilde{t}} d\tilde{t} \quad (A.5)$$

The time lag is determined at steady state, so the next steps evaluate each term as time goes to infinity. At steady state, the concentration profile becomes linear and the radius, a, of the core of every oxidized particle approaches 0, except at the downstream boundary. Using the cumulative oxygen permeate defined in Eq. (26) and evaluating each term, Eq. (A.5) becomes

$$\int_0^1 \tilde{x}(1-\tilde{x})\,d\tilde{x} + \frac{\phi\beta}{C_m(0)}\int_0^1 \tilde{x}\,d\tilde{x} = -\frac{Q_{t,ss}}{6(\mathrm{Flux})_{ss}C_m(0)} + \tilde{t} \quad (A.6)$$

$$\frac{1}{6} + \frac{1}{2}\frac{\phi\beta}{C_m(0)} = -\frac{Q_{t,ss}}{6(\mathrm{Flux})_{ss}\theta_0} + \tilde{t} \quad (A.7)$$

The time lag is determined by finding the point where the steady-state asymptote of the cumulative permeate crosses the time axis, i.e., by setting $Q_{t,ss} = 0$ in Eq. (A.7), to get

$$\theta = \theta_0\left(1 + \frac{3\phi\beta}{C_m(0)}\right). \quad (A.8)$$

Nomenclature

a	radius of the unreacted core, see Fig. 1
C_m	oxygen concentration in matrix polymer
C_p	oxygen concentration in oxidized scavenging polymer
Da	Damköhler number
D_m	diffusion coefficient for oxygen in matrix polymer
D_p	diffusion coefficient for oxygen in oxidized scavenging polymer
H	partition coefficient, S_m/S_p
k	oxidation rate parameter
L	film thickness
p_{O_2}	oxygen partial pressure
P	oxygen permeability coefficient
Q_t	cumulative amount of oxygen permeate
R	scavenging polymer particle radius
S_m	solubility coefficient for oxygen in matrix polymer
S_m, S_p	solubility coefficient for oxygen in oxidized scavenging polymer
t	time
x	position in film
$\sim$	denotes dimensionless variables (see Eq. (18))

Greek letters

β	oxygen scavenging capacity, moles O_2/cm^3 OSP
Δ	D_p/D_m
ε	R/L
ϕ	volume fraction of scavenging polymer
θ	time lag with scavenging
θ_0	time lag without scavenging
$\rho_{polymer}$	density of scavenging polymer

References

[1] K.F. Finger, A.P. Lemberger, T. Higuchi, L.W. Busse, D.E. Wursten, Investigation and development of protective ointments. IV The influence of active fillers on the permeability of semisolids, J. Am. Pharm. Assoc. 49 (1960) 569–573.
[2] D.R. Paul, The effect of immobilizing adsorption on the diffusion time lag, J. Polym. Sci. 7A-2 (1969) 1811–1818.
[3] D.R. Paul, D.R. Kemp, The diffusion time lag in polymer membranes containing adsorptive fillers, J. Polym. Sci. 41C (1973) 79–93.
[4] D.R. Paul, W.J. Koros, Effect of partially immobilizing sorption on permeability and the diffusion time lag, J. Polym. Sci., Polym. Phys. Ed. 14 (1976) 675–685.
[5] M.A. Cochran, R. Folland, J.W. Nicholas, E.R. Robinson, Packaging, U.S. Patent 5,021,515 (1991), assigned to CMB Foodcan.
[6] D.V. Speer, C.R. Morgan, W.P. Roberts, Methods and compositions for oxygen scavenging, U.S. Patent 5,211,875 (1993), assigned to W.R. Grace.
[7] D.V. Speer, W.P. Roberts, C.R. Morgan, A.W. VanPutte, Multilayer structure for a package for scavenging oxygen, U.S. Patent 5,529,833 (1996), assigned to W.R. Grace.
[8] K. Katsumoto, T.Y. Ching, Multi-component oxygen scavenging composition, U.S. Patent 5,776,361 (1998), assigned to Chevron Chemical Company.
[9] T.A. Blinka, F.B. Edwards, N.R. Miranda, D.V. Speer, J.A. Thomas, Zeolite in packaging film, U.S. Patent 5,834,079 (1998), assigned to W.R. Grace.
[10] P.J. Cahill, S.Y. Chen, Oxygen scavenging condensation copolymers for bottles and packaging articles, U.S. Patent 6,083,585 (2000), assigned to BP Amoco Corporation.
[11] M.E. Stewart, R.N. Estep, B.B. Gamble, M.D. Clifton, D.R. Quillen, L.S. Buehrig, V. Govindarajan, M.J. Dauzvardis, Blends of oxygen scavenging polyamides with polyesters which contain zinc and cobalt, U.S. Patent Application Publication US 2006/0148957 (2006), assigned to Constar International Inc., Eastman Chemical Company.
[12] A.V. Tobolsky, D.J. Metz, R.B. Mesrobian, Low temperature autoxidation of hydrocarbons: the phenomenon of maximum rates, J. Am. Chem. Soc. 72 (1950) 1942–1952.
[13] R.G. Bauman, S.H. Maron, Oxidation of polybutadiene. I. Rate of oxidation, J. Polym. Sci. 22 (1956) 1–12.
[14] S.W. Beavan, D. Phillips, Mechanistic studies on the photo-oxidation of commercial poly(butadiene), Eur. Polym. J. 10 (1974) 593–603.
[15] J.F. Rabek, J. Lucki, B. Rånby, Comparative studies of reactions of commercial polymers with molecular oxygen, singlet oxygen, atomic oxygen and ozone-I, Eur. Polym. J. 15 (1979) 1089–1100.
[16] V.B. Ivanov, S.G. Burkova, Y.L. Morozov, V.Y. Shlyapintokh, Kinetics of the chain-propagation and chain-termination reactions in the oxidation of polybutadiene and copolymers of butadiene with styrene, Kinetika i Kataliz 20/5 (1979) 1330–1333.
[17] C. Adam, J. Lacoste, J. Lemaire, Photo-oxidation of elastomeric materials. Part 1-photo-oxidation of polybutadienes, Polym. Degrad. Stab. 24 (1989) 185–200.
[18] M. Piton, A. Rivaton, Photooxidation of polybutadiene at long wavelengths ($\lambda > 300$ nm), Polym. Degrad. Stab. 53 (1996) 343–359.
[19] R.A. Sheldon, J.K. Kochi, Metal-catalyzed Oxidations of Organic Compounds, Academic Press, New York, 1981.
[20] C.D. Mueller, S. Nazarenko, T. Ebeling, T.L. Schuman, A. Hiltner, E. Baer, Novel structures by microlayer coextrusion—Talc-filled PP, PC/SAN, and HDPE/LLDPE, Polym. Eng. Sci. 37/2 (1997) 355–362.
[21] C. Yang, E.E. Nuxoll, E.L. Cussler, Reactive barrier films, AIChE J. 47/2 (2001) 295–302.
[22] C. Yang, E.L. Cussler, Oxygen barriers that use free radical chemistry, AIChE J. 47/12 (2001) 2725–2732.
[23] N.K. Lape, C. Yang, E.L. Cussler, Flake-filled reactive membranes, J. Membr. Sci. 209 (2002) 271–282.
[24] R.A. Siegel, E.L. Cussler, Reactive barrier membranes: some theoretical observations regarding the time lag and breakthrough curves, J. Membr. Sci. 229 (2004) 33–41.
[25] R.A. Siegel, E.L. Cussler, Layered reactive barrier films, J. Membr. Sci. 252 (2005) 29–36.
[26] E.E. Nuxoll, E.L. Cussler, The third parameter in reactive barrier films, AIChE J. 51/2 (2005) 456–463.
[27] S.E. Solovyov, A.Y. Goldman, Theory of transient permeation through reactive barrier films I. Steady state theory for homogeneous passive and reactive media, Int. J. Polym. Mat. 54 (2005) 71–91.
[28] S.E. Solovyov, A.Y. Goldman, Theory of transient permeation through reactive barrier films II. Two layer reactive-passive structures with dynamic interface, Int. J. Polym. Mat. 54 (2005) 93–115.
[29] S.E. Solovyov, A.Y. Goldman, Theory of transient permeation through reactive barrier films III. Solute ingress dynamics and model lag times, Int. J. Polym. Mat. 54 (2005) 117–139.
[30] S.E. Solovyov, A.Y. Goldman, Optimized design of multilayer barrier films incorporating a reactive layer I. Methodology of ingress analysis, J. Appl. Polym. Sci. 100 (2006) 1940–1951.
[31] S.E. Solovyov, A.Y. Goldman, Optimized design of multilayer barrier films incorporating a reactive layer II. Solute dynamics in two-layer films, J. Appl. Polym. Sci. 100 (2006) 1952–1965.
[32] S.E. Solovyov, A.Y. Goldman, Optimized design of multilayer barrier films incorporating a reactive layer III. Case analysis and generalized multilayer solutions, J. Appl. Polym. Sci. 100 (2006) 1966–1977.
[33] S.E. Solovyov, A.Y. Goldman, Mass Transport Reactive Barriers in Packaging, DEStech Publications, Lancaster, PA, 2008.
[34] K.T. Gillen, R.L. Clough, Rigorous experimental confirmation of a theoretical model for diffusion-limited oxidation, Polymer 33/20 (1992) 4358–4365.
[35] L.M. Rincon-Rubio, B. Fayolle, L. Audouin, J. Verdu, A general solution of the closed-loop kinetic scheme for the thermal oxidation of polypropylene, Polym. Degrad. Stab. 74 (2001) 177–188.
[36] M. Coquillat, J. Verdu, X. Colin, L. Audouin, R. Nevière, Thermal oxidation of polybutadiene. Part 1: Effect of temperature, oxygen pressure and sample thick-

ness on the thermal oxidation of hydroxyl-terminated polybutadiene, Polym. Degrad. Stab. 92 (2007) 1326–1333.
[37] M. Coquillat, J. Verdu, X. Colin, L. Audouin, R. Nevière, Thermal oxidation of polybutadiene. Part 2: Mechanistic and kinetic schemes for additive-free non-crosslinked polybutadiene, Polym. Degrad. Stab. 92 (2007) 1334–1342.
[38] M. Coquillat, J. Verdu, X. Colin, L. Audouin, R. Nevière, Thermal oxidation of polybutadiene. Part 3: Molar mass changes of additive-free non-crosslinked polybutadiene, Polym. Degrad. Stab. 92 (2007) 1343–1349.
[39] H. Li, D.K. Ashcraft, B.D. Freeman, M.E. Stewart, M.K. Jank, T.R. Clark, Non-invasive headspace measurement for characterizing oxygen scavenging in polymers, Polymer 49 (2008) 4541–4545.
[40] H. Li, D.K. Ashcraft, K. Tung, B.D. Freeman, M.E. Stewart, J. Jenkins, Characterization of oxygen scavenging membranes based on commercial polybutadiene, submitted for publication.
[41] J. Crank, The Mathematics of Diffusion, 2nd Ed., Oxford University Press, Oxford, 1975.
[42] D.R. Paul, C.B. Bucknall (Eds.), Polymer Blends, vol. 1, Formulation, John Wiley, New York, 2000.
[43] A. Polyakova, R.Y.F. Liu, D.A. Schiraldi, A. Hiltner, E. Baer, Oxygen-barrier properties of copolyesters based on ethylene terephthalate, J. Polym. Sci.: Part B: Polym. Phys. 39 (2001) 1889–1899.
[44] K. Hodge, T. Prodpran, N.B. Shenogina, S. Nazarenko, Diffusion of oxygen and carbon dioxide in thermally crystallized syndiotactic polystyrene, J. Polym. Sci.: Part B: Polym. Phys. 39 (2001) 2519–2538.
[45] C. Maxwell, Treatise on Electrical and Magnetism, vol. I, Oxford University Press, London, p. 365.
[46] H.L. Frisch, The time lag in diffusion, J. Phys. Chem. 61 (1957) 93–95.